Journal of Statistical Physics, Vol. 57, Nos. 1/2, 1989

Renormalization Group Studies of the Ashkin–Teller Model

Paulo Murilo C. de Oliveira[1] and F. C. Sá Barreto[2]

Received January 5, 1989; revision received May 29, 1989

The two-and-three-dimensional Ashkin–Teller model is studied within two renormalization group treatments. The complete flow diagram is obtained for this two-parameter Hamiltonian and the results for the critical couplings and critical exponents are compared to the exact ones when avaible.

KEY WORDS: Ising models; Real Space RG.

1. INTRODUCTION

The Ashkin–Teller (AT) model has four states per lattice site and has been introduced[1] as a generalization of the Ising model to describe a four-component system. The AT model can be expressed as two Ising models coupled by a four-spin interaction.[2,3] Each site i is occupied by two spins σ_i and S_i, both represented by Boolean variables. By combining these two variables, we obtain four possible states on each site. The AT Hamiltonian is defined as

$$\beta H = \sum_{\langle i,j \rangle} 2\{J(\sigma_i \otimes \sigma_j + S_i \otimes S_j) + K(\sigma_i \otimes S_i \otimes \sigma_j \otimes S_j)\} \tag{1}$$

where $\beta = (kT)^{-1}$ and J and K stand for the two- and four-spin couplings, respectively. The sum is over nearest neighbor pairs $\langle i,j \rangle$, and $\otimes$ is the XOR (exclusive-or) Boolean operator. The four-spin coupling term can also be interpreted as an Ising ordinary two-spin coupling between the

[1] Instituto de Física, Universidade Federal Fluminense, Niterói RJ 24000, Brazil.
[2] Departamento de Física, Universidade Federal de Minas Gerais, Belo Horizonte MG 30000, Brazil.

0022-4715/89/1000-0053$06.00/0

composed spins $\sigma \otimes S$ that can be defined at each site. The factor 2 appears because we choose the two-parallel-spin configuration as the zero level for the energy measure, instead of the usual choice of $\pm J$ energy for parallel and antiparallel configurations. The 2D AT model has not been solved exactly, but some of its critical behavior is known.[3-5] At $K=0$ the model reduces to two decoupled Ising models with nearest neighbor interaction J. For $J=K$ the model reduces to the four-state Potts model. These two limiting models show second-order phase transitions, but with different critical indices. The two critical points associated with these two limits are connected by a line of continuously varying critical indices. Wegner[6] showed that the 2D critical AT model is equivalent to a staggered eight-vertex model, and since then relations between the critical indices of these two models have been derived.[7-9] A 1D quantum (time-continuous) Hamiltonian analog of the 2D AT model has been studied by different methods[10,11] and the validity of the previously mentioned extended relations has been established. For the 3D AT model only few mean-field, series, and Monte Carlo results are available.[12,13]

In this paper we present a study of the critical properties of the 2D and 3D AT models within two similar approaches. In the first one we revise the mean-field renormalization group (MFRG) treatment of the model presented previously.[14] This revision is based on two aspects. (a) We used two coupled recursion relations to obtain the complete (J, K) flow diagram, instead of the only one parametrized recursion relation used in ref. 14, which leads to restricted only-J-varying independent flow diagrams. (b) We have used larger finite lattices, improving substantially the results. The second approach is based on the simultaneous use of three different finite-sized lattices to obtain the renormalization group recursion relations. This approach, which has been successfully used to study the Ising and three-state Potts models,[15] eliminates the weakness of the only-two-lattice approach[16]—the mean field assumption that the order parameter scales in the same rate as the boundary field—and furnishes excellent results even for small lattices.

2. GENERAL FORMALISM

We define the AT model in a finite, d-dimensional lattice with N sites. Each site i contains two Ising spins σ_i and S_i which can assume values 0 and 1. The model Hamiltonian is

$$\beta H = 2J \sum_{\langle i,j \rangle} (\sigma_i \otimes \sigma_j + S_i \otimes S_j) + 2K \sum_{\langle i,j \rangle} \sigma_i \otimes S_i \otimes \sigma_j \otimes S_j + 2hJ \sum_i p_i(\sigma_i + S_i) + 2gK \sum_i p_i(\sigma_i \otimes S_i) \tag{2}$$

where $i = 1, 2, \ldots, N$, and $\langle i, j \rangle$ are nearest neighbor pairs. This model corresponds to a finite lattice isolated from an infinite one, by cutting the boundary links in between. The fields $2hJ$ and $2gK$, representing the vanishing interactions between sites inside and outside isolated part of the lattice, are included in order to break the spin-flip symmetry. The weight p_i is the number of cut boundary links at site i—internal sites have $p_i = 0$. For a given configuration c of the spins σ_i and S_i, let us define

$$M_c \equiv \sum_i (\sigma_i + S_i) \tag{3a}$$

$$T_c \equiv \sum_i p_i(\sigma_i + S_i) \tag{3b}$$

$$Q_c \equiv \sum_i \sigma_i \otimes S_i \tag{3c}$$

$$R_c \equiv \sum_i p_i(\sigma_i \otimes S_i) \tag{3d}$$

If $\langle \cdots \rangle_0$ denotes thermodynamic average for $h = g = 0$, we have $\langle M_c \rangle_0 = 2\langle Q_c \rangle_0 = N$ and $\langle T_c \rangle_0 = 2\langle R_c \rangle_0 = P \equiv \sum p_i$.

Up to first order in the fields h and g, we get the finite lattice order parameters M and Q,

$$M = \langle M_c \rangle - \langle M_c \rangle_0 = -2\beta hJ(\langle M_c T_c \rangle_0 - NP) \tag{4a}$$

$$Q = \langle Q_c \rangle - \langle Q_c \rangle_0 = -2\beta gK(\langle Q_c R_c \rangle_0 - NP/4) \tag{4b}$$

3. TWO-LATTICE MFRG

The MFRG assumption is that the ratio between each of those order parameters and the corresponding field does not depend upon the length scale for large linear sizes $L = N^{1/d}$. The plausibility mean-field argument to sustain this assumption is to invoke the magnetization of the outside lattice as the physical origin for the fields h and g acting on the inside finite lattice. In this case, M and h in Eq. (4a) must scale as L^{φ}, both with the same unknown exponent φ. The same occurs also for Q and g in Eq. (4b). As a consequence, the quantities $JF_L(x, y)$ and $KW_L(x, y)$—defined below as functions of $x \equiv \exp(-2J)$ and $y \equiv \exp(-2K)$—scale as L^0, i.e., they do not depend upon the lattice size L, in the large-L limit,

$$F_L(x, y) = 2(\langle M_c T_c \rangle_0 - NP)/N \tag{5a}$$

$$W_L(x, y) = (4\langle Q_c R_c \rangle_0 - NP)/N \tag{5b}$$

The numerical factors in Eq. (5) are convenient for dealing only with whole numbers in the computer. The MFRG recursion relations

$$J'F_{L'}(x', y') = JF_L(x, y) \tag{6a}$$

$$K'W_{L'}(x', y') = KW_L(x, y) \tag{6b}$$

are obtained by equating the values of JF and KW computed for two different sized finite lattices with lengths $L' < L$. From these relations one obtains the complete flow diagram in (J, K) space of parameters. In order to solve numerically Eq. (6) for J' and K', given J and K, we used the method of iteration (see, for instance, ref. 17).

Using the smallest possible finite square lattices, namely the ones with $N = 2$ and $N' = 1$ yielding a scaling factor $b = L/L' = \sqrt{2}$, we obtained the phase diagram shown in Fig. 1a for the $J > 0$ and $K > 0$ case, where we used the variables *tanh J* and *tanh K* in order to show all the fixed points. For $K < 0$, we adopted a staggered g field, reaching a different version of Eq. (6b), and obtained the remainder of the phase diagram shown in Fig. 1b—the $J < 0$ part is symmetric to the whole picture. Although each part of the diagram is obtained by a different set of RG recursion relations, they must be interpreted as a whole. There are four stable fixed points (solid, tilted squares) whose basins of attraction correspond to the four possible thermodynamic phases:

(i) P (or $\tilde{\text{P}}$) for the paramagnetic phase where there is no magnetic order at all, and both M and Q vanish.

(ii) F for the ferromagnetic Ising phase where the composed spins $\sigma \otimes S$ are ferromagnetically ordered ($Q \neq 0$) but neither σ or S spins solely present order ($M = 0$).

(iii) $\tilde{\text{F}}$ for the antiferromagnetc Ising phase similar to F.

(iv) X (or $\tilde{\text{X}}$) for the Baxter phase where σ, S, and $\sigma \otimes S$ are ordered ($M \neq 0$ and $Q \neq 0$).

Figure 1 presents also four semistable fixed points (solid circles) of interest for the study of the critical behavior:

(i) A (or $\tilde{\text{A}}$), where the ferro–para ordinary Ising transition occurs for both σ and S spins independently, in the absence of the four-spin interaction.

(ii) B, where the ferro–para Ising transition occurs for the composed spins $\sigma \otimes S$.

(iii) $\tilde{\text{B}}$, where the antiferro–para Ising transition occurs, similar to B.

(iv) D, where a fourth Ising transition occurs. In the $K \to \infty$ limit, the

$\sigma \otimes S$ spins are completely frozen in the ferromagnetic ground state, but the pairs σS can flip together at each site, allowing the quoted transition. It appears just at half the normal Ising critical J value, because there are two J bonds linking neighboring sites.

The most interesting critical behavior of the AT model corresponds to the last two fixed points that are completely unstable:

(i) C, where the four-state Potts model transition occurs.

(ii) E, where the phases $\tilde{F}$ and X degenerate.

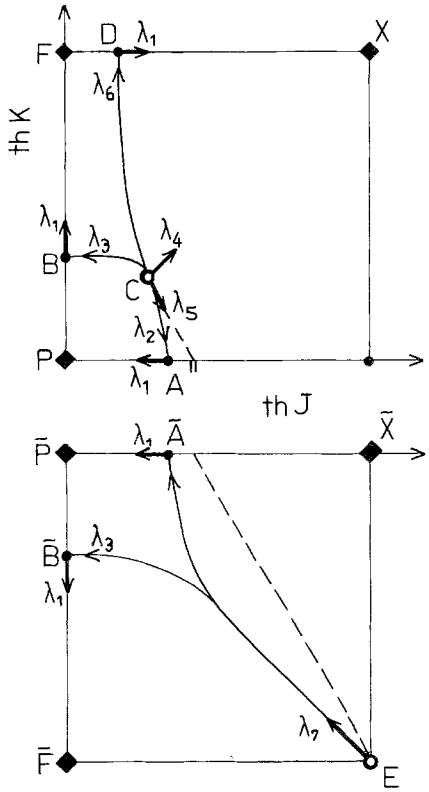

Fig. 1. The RG phase diagram obtained from the smallest possible finite lattices with $N = 2$ and $N' = 1$, in 2D. The qualitative features are the same for all other lattice sizes and also for the three-lattice approach. The quantitative results are systematically improved, however, as can be seen from the tables. The arrows indicate the RG eigenvectors at fixed points, and the various λ's indicate the respective eigenvalues. Solid, tilted squares are RG attractors corresponding to thermodynamic phases, open circles are completely unstable critical fixed points governing crossover behavior, and solid circles are the critical semistable fixed points governing critical behavior along critical lines. The dashed E–C line shows the exactly known nonuniversal transition. Near this line, the pair of points marked on the J axis correspond to our best results obtained from the RG defined in Section 4.

Line E–C is known to have nonuniversal behavior, with continuously varying critical exponents along it. Within RG theory, a line of fixed points can fit this feature. Although our flow diagram of Fig. 1 does not present such a line of fixed points, this goal is approached by taking larger finite lattices, and furthermore by relaxing the MFRG assumption (see next section). For now, we analyze the correct aspects of Fig. 1. First, the eigenvalue $\lambda_7 = 1$ corresponds to the quoted line of fixed points, beginning at point E. At $T=0$, the X–F transition occurs at $K=-J$. We can understand this fact by analyzing the two competing ground states of Hamiltonian (1) for $J>0$ and $K<0$: each of the three terms $\sigma_i \otimes \sigma_j$, $S_i \otimes S_j$, and $(\sigma_i \otimes \sigma_j) \otimes (S_i \otimes S_j)$—note that we have regrouped the four-spin term in a convenient new way—can assume values 0 or 1. Under the point of view of the $J>0$ interaction, it is energetically convenient to take the 0 result for both the first two $\otimes$ terms above. Under the point of view of the $K<0$ interaction, however, it is convenient to take value 1 for one of them and 0 for the other: this saves an amount $-K$ (absolute value) of energy, paying a price J. The transition from one ground state to the other occurs then at $J=-K$, in agreement with the finite slope shown near point E. The deviation between our curve and the exact one is magnified because we decided to draw them in a *tanh* scale: actually, the exact curve corresponds to $2K=-2J+2$, near E. The extra term 2 is negligible in the limit $T \to 0$ (or $J, -K \to \infty$), and is due to the doubled degeneracy of the possible excitations from the X ground state relative to the corresponding excitations from the $\tilde{\mathrm{F}}$ one: by flipping only one spin from the X ground state, we have a choice between spins σ_i or S_i to localize the frustrated J bonds, but we have no such choice by flipping one spin from the $\tilde{\mathrm{F}}$ ground state in order to get a first excited state.

The four-state Potts fixed point C is located at the exactly known position $J_C = K_C = (\ln 3)/4$ and the symmetries of Hamiltonian (1) are also respected there: one eigenvector along the $J=K$ axis governing the Potts criticality, and the other with exactly -2 slope. This value can be understood as follows: starting from critical point C, where the three spin couplings of Hamiltonian (1) are equivalent, and increasing J by a small quantity δ, it is necessary to decrease K by 2δ in order to restore criticality, because there are two Ising J couplings and only one K counterpart. Other symmetries are also respected at points A, $\tilde{\mathrm{A}}$, B, $\tilde{\mathrm{B}}$, and D, namely $J_A = K_B = -K_{\tilde{B}} = 2J_D$, and right angles between eigenvectors at B, $\tilde{\mathrm{B}}$, and D.

Besides the qualitative aspects discussed up to now, Table I summarizes the numerical results we get using bigger lattices for $J, K>0$. Note, in particular, the clear tendency to unity presented by eigenvalues λ_2 and λ_5 along line E–C, according to its nonuniversal character.

For the 3D AT model, the phase diagram also presents the same

Table I. Square Lattice AT Model[a]

N	N'	J_A	ν_I	ν_P	λ_2	λ_3	λ_5	λ_6
2	1	0.3466	1.67	1.43	0.83	0.75	1.14	0.67
4	2	0.3699	1.28	1.03	0.81	0.67	1.16	0.75
9	6	0.3861	1.18	0.94	0.88	0.80	1.09	0.83
Exact		0.4407	1	0.67	1		1	

[a] MFRG results for Ising critical couplings $J_A = K_B = -K_{\bar{B}} = 2J_D$, values of Ising ($\nu_I \equiv \ln b/\ln \lambda_1$) and Potts ($\nu_P \equiv \ln b/\ln \lambda_4$) correlation length critical exponents, and eigenvalues λ_2, λ_3, λ_5, and λ_6. The exactly known Potts critical coupling $J_C = K_C = (\ln 3)/4$ (see Fig. 1a) is obtained for all lattice sizes (with minor deviations for $N = 9$).

features of Fig. 1 for $K > 0$, but there is a fundamental difference for $K < 0$, as shown in Fig. 2 obtained from the same lattices $N = 2$ and $N' = 1$. Now, point E is located at a finite temperature, and the paramagnetic phase is not extended until zero temperature along the $J = K$ axis, as in 2D. This behavior agrees with results obtained from series and Monte Carlo data[12] (see Figs. 1 and 3 of that reference). Furthermore, the eigenvalues λ_8 and λ_9 are no longer equal to 1 (for $N = 2$ and $N' = 1$, we get $\lambda_8 = 1.28$ and $\lambda_9 = 1.11$), and line E–C no longer has the nonuniversal character presented in 2D, also in agreement with ref. 12. At point $\tilde{E}$, we get two eigenvalues, one smaller than 1 responsible for its attraction character. The other eigenvalue is ∞, and gives the runaway behavior characteristic of a first-order phase transition along line E–$\tilde{E}$, also in agreement with ref. 12.

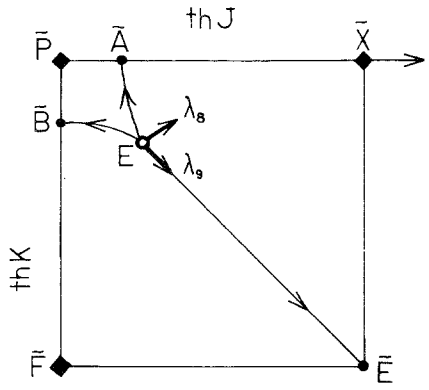

Fig. 2. The $K < 0$ RG phase diagram for 3D. For $K > 0$, the diagram is similar to the upper part of Fig. 1.

Table II. 3D AT Model: MFRG Results

N	N'	J_A	J_C	ν_I	ν_P	λ_2	λ_3	λ_5	λ_6
8	1	0.2066	0.1713	1.22	1.04	0.59	0.50	1.48	0.25
8	2	0.2077	0.1708	1.11	0.93	0.68	0.60	1.33	0.42
8	4	0.2091	0.1701	0.99	0.82	0.81	0.75	1.17	0.67
Series[18]		0.2168	0.1616	0.63					

We did not obtain the phase $\langle \sigma \rangle$ proposed in ref. 12, where the symmetry between spins σ and S is spontaneously broken, but even the existence of this phase is an open question, and our results are also inconclusive about this point because we did not introduce any symmetry-breaking ingredient between spins σ and S. Numerical results for $K > 0$ are shown in Table II, for bigger lattices. Unfortunately, we are not able to do calculations for sufficiently large lattices in order to be conclusive about the critical behavior in this 3D case, but some qualitative features can be observed: for instance, the tendency to obtain $\lambda_2 > 1$ for larger lattices, as expected.

4. THREE-LATTICE RG

As we pointed out, the assumption that the symmetry-breaking fields (boundary fields h and g) scale in the same form as the order parameters (bulk magnetizations M and Q, respectively) is incorrect. In this section we abandon this assumption, allowing for different scaling exponents. Thus, in the large-L limit, the ratios M/h and Q/g scale as L^{φ} and L^{ϕ}, respectively, where φ and ϕ are some unknown exponents. Let us consider three lattices of sizes L, L', and L'' ($L > L' > L''$). At some fixed critical point $(x^*, y^*) = (\exp(-2J^*), \exp(-2K^*))$ we can write

$$J^* F_{L''}(x^*, y^*)\, L''^{-\varphi} = J^* F_{L'}(x^*, y^*)\, L'^{-\varphi} \tag{7a}$$

$$J^* F_{L'}(x^*, y^*)\, L'^{-\varphi} = J^* F_{L}(x^*, y^*)\, L^{-\varphi} \tag{7b}$$

$$K^* W_{L''}(x^*, y^*)\, L''^{-\phi} = K^* W_{L'}(x^*, y^*)\, L'^{-\phi} \tag{7c}$$

$$K^* W_{L'}(x^*, y^*)\, L'^{-\phi} = K^* W_{L}(x^*, y^*)\, L^{-\phi} \tag{7d}$$

Eliminating φ an ϕ from this set of equations, we can determine the possible solutions for (J^*, K^*). Choosing one of them, we can write the recursion relations

$$J'F_{L'}(x', y') = \frac{F_{L'}(x^*, y^*)}{F_L(x^*, y^*)} JF_L(x, y) \tag{8a}$$

$$K'W_{L'}(x', y') = \frac{W_{L'}(x^*, y^*)}{W_L(x^*, y^*)} KW_L(x, y) \tag{8b}$$

There is a trivial solution to choose for the fixed point (J^*, K^*), namely $J^* = K^* = J_C = K_C$, the location of point C (see Fig. 1). This choice reproduces the same results already obtained from the MFRG approach presented in Section 3. Another interesting possible choice is $J^* = J_A$, $K^* = 0$, where J_A remains to be determined from Eq. (7a) and (7b). In this case, however, the ratio

$$\frac{W_{L'}(x^*, y^*)}{W_L(x^*, y^*)}$$

appearing in Eq. (8b) cannot be determined from (7d). Then, we choose it by imposing the symmetry $K_B = J_A$ in the resulting flow diagram. Giving support to this choice, we observe that all other symmetries quoted in Section 3 are recovered.

Numerical values are presented in Table III, and values for J_A and ν_I reproduce that obtained for the Ising model.[15] We see that results for both critical couplings and critical indices improve over those presented in Table I. It is interesting to note that the only source of inaccuracy the present method still has is the small size of the finite lattices we used: the only assumption now is the finite-size power-law behavior supposed for thermodynamic quantities near criticality. The absence of the erroneous mean-field hypothesis characteristic of the two-lattice approach yields very good numerical results even for the small lattices we used here.

Table III. Square Lattice AT Model[a]

N	N'	N''	J_A	J_C	ν_I	ν_P	λ_2	λ_5
4	2	1	0.4093	0.2963	1.23	0.98	0.82	1.15
9	4	1	0.4482	0.2919	1.14	0.87	0.84	1.14
12	6	2	0.4167	0.2795	1.08	0.83	0.83	1.14
12	9	6	0.4304	0.2919	0.95	0.68	0.91	1.06
	Exact		0.4407	0.2747	1	0.67	1	1

[a] Three-lattice RG results. Periodic boundary conditions are adopted in one direction of the finite lattices, except for the first row.

5. CONCLUDING REMARKS

In this communication we have studied the 2D and 3D Ashkin–Teller model by two RG approaches. An improved version of the two-lattice renormalization scheme overcomes the incorrect qualitative results obtained in ref. 14, where only J is allowed to vary by the scaling transformation, while K is considered as a fixed parameter. By exploring the scaling behavior of two order parameters M and Q, we obtain a complete two-dimensional flow diagram in (J, K) space. This improvement is important because it allows the study of crossover behavior, in particular the non-universal character observed in the 2D AT model. Various exactly known critical quantities and symmetries are recovered by this simple approach.

However, this two-lattice RG is based on an incorrect assumption: that each order parameter M or Q scales with the lattice size L through the same exponent as the respective symmetry-breaking field h or g. This fact limits numerical accuracy. In order to overcome this source of incorrectness, we introduce another RG without the quoted assumption, using three instead of two lattices to define the recursion relations. This last approach has the same status of the usual finite-size scale hypothesis, having no other assumptions, the only limit for accuracy being the computational capability for large-lattice calculations. Remember that the only assumption behind this approach is that any thermodynamic quantity scales as a power law of the system length size, or, in other words, that the thermodynamic potentials are generalized homogeneous functions of the corresponding fields ($J-J_C$ and $K-K_C$ in the present case) and *also* of the inverse length size (L^{-1}) of the system. Even for lattices of at most 12 sites, we were able to obtain good results with errors of a few percent. Improved results can be obtained by using Monte Carlo methods to calculate the averages in Eq. (4). Work along this line is in course.

Finally, we must point out that for the first time within the MFRG scheme a more-than-one-parameter Hamiltonian has been correctly treated once the complete flow diagram has been obtained, allowing the study of crossover behavior. Other models, e.g., the Blume–Emery–Griffiths model, can be treated in the same scheme. Work along this line is also in course.

ACKNOWLEDGMENTS

One of the authors (F.C.S.B.) is grateful to the Department of Physics, Harvard University, where the manuscript was written. We are also grateful to both referees for comments about the $K<0$ part of the phase diagram in 3D. This work was supported by CNPq, FINEP, and CAPES (Brazil).

REFERENCES

1. J. Ashkin and E. Teller, *Phys. Rev.* **64**:178 (1943).
2. C. Fan, *Phys. Lett.* **39A**:136 (1972).
3. C. Fan and F. Y. Wu, *Phys. Rev.* **B2**:723 (1970).
4. H. J. F. Knops, *J. Phys. A* **8**:1508 (1975).
5. R. J. Baxter, *Exactly Solved Models in Statistical Mechanics* (Academic Press, New York, 1982), Chapter 12.
6. F. Wegner, *J. Phys. C* **5**:L131 (1972).
7. I. Enting, *J. Phys. A* **8**:L35 (1975).
8. L. Kadanoff, *Ann. Phys.* (NY) **120**:39 (1979).
9. L. Kadanoff and A. Brown, *Ann. Phys.* (NY) **121**:318 (1979).
10. M. Kohmoto, M. den Nijs, and L. Kadanoff, *Phys. Rev. B* **24**:5229 (1981).
11. F. C. Alcaraz and J. R. Drugowich de Felicio, *J. Phys. A* **17**:L651 (1984).
12. R. V. Ditzian, R. J. Banavar, G. S. Grest, and L. Kadanoff, *Phys. Rev. B* **22**:2542 (1980).
13. P. L. Christiano and S. Goulart Rosa, Jr., *Phys. Lett.* **110A**:44 (1985).
14. J. A. Plascak and F. C. Sá Barreto, *J. Phys. A* **19**:2195 (1986).
15. J. O. Indekeu, A. Maritan, and A. C. Stella, *Phys. Rev. B* **35**:305 (1987).
16. J. O. Indekeu, A. Maritan, and A. C. Stella, *J. Phys. A* **15**:L291 (1982).
17. B. P. Demidovich and I. A. Maron, *Computational Mathematics* (MIR, Moscow, 1978), Chapter 8.
18. F. Y. Wu, *Rev. Mod. Phys.* **54**:235 (1982).